




Designing Soft Pneumatic Actuators for Thumb Movements

Yuanyuan Wang , Shota Kokubu, Zhongchao Zhou, Xinyao Guo, Ya-Hsin Hsueh , and Wenwei Yu 

Abstract—Studies have developed various types of soft robotic gloves for hand rehabilitation in recent years. Most soft actuators achieved a sufficient thumb flexion assist while lacking opposition support, which requires the coordination of thumb flexion and abduction-adduction. The difficulties for thumb support lie in the intrinsic complexity of thumb movements and spatial restriction of the hand. To realize multiple degrees of freedom of the thumb and make effective use of the limited space of the hand's dorsal side, we optimized and compared two approaches for thumb support. The combination approach used two independent soft actuators for thumb flexion and abduction-adduction support, respectively. The all-in-one approach used one single soft actuator to assist motions in different directions. We designed the soft actuators for each approach based on the thumb's biomechanical characteristics and evaluated their thumb flexion, abduction support performance in terms of the range of motion (RoM) and force output, and the opposition support performance using an enhanced Kapandji test. The results showed a larger abduction RoM and force output of the combination approach and a higher Kapandji score of the all-in-one approach, indicating that the two approaches might be applicable for thumb support but have the advantage in different rehabilitation stages.

Index Terms—Soft robot applications, rehabilitation robotics, thumb opposition, enhanced Kapandji test.

I. INTRODUCTION

OVER 80 million people currently live have experienced a stroke, and the number is increasing rapidly [1]. Hand recovery after stroke might be a challenging and lengthy process due to the complexity of finger movements. Also, due to the labor shortage in rehabilitation therapists, it becomes necessary to use an assistive device to achieve the required high repetition for hand rehabilitation.

Researchers have developed various hand rehabilitation gloves driven by either rigid systems or soft pneumatic actuators.

Manuscript received April 13, 2021; accepted July 24, 2021. Date of publication August 18, 2021; date of current version September 14, 2021. This letter was recommended for publication by Associate Editor H. Su and Editor K.-J. Cho upon evaluation of the reviewers' comments. This work was supported by JSPS grant-in-aid for scientific research (b) 19K22949. (*Corresponding author: Wenwei Yu.*)

Yuanyuan Wang, Shota Kokubu, Zhongchao Zhou, and Xinyao Guo are with the Graduate School of Science and Engineering, Chiba University, Chiba 2638522, Japan (e-mail: dakiso2017@gmail.com; s.kokubu@chiba-u.jp; zhouzhongchao@outlook.com; guoxinyao1991@gmail.com).

Ya-Hsin Hsueh is with the Department of Electronic Engineering, National Yunlin University of Science and Technology, Yunlin County 64002, Taiwan (e-mail: hsuehyh@yuntech.edu.tw).

Wenwei Yu is with the Center for Frontier Medical Engineering, Chiba University, Chiba 2638522, Japan (e-mail: yuwill@faculty.chiba-u.jp).

This article has supplementary downloadable material available at <https://doi.org/10.1109/LRA.2021.3105799>, provided by the authors.

Digital Object Identifier 10.1109/LRA.2021.3105799

The rigid systems [2]–[4] depend on servomotors or pneumatic pressure to produce pulling of linkages and cables that are connected to finger segments, making them uncomfortable for long-term use and being easier to induce fatigue of joints. On the other hand, soft pneumatic actuators made from elastomeric materials have been widely applied in rehabilitation gloves in recent years. Some studies [5]–[7] utilized the intrinsic traits of the elastomeric material and unique geometrical design (PneuNet) to realize the bending of actuators. Others [8], [9] used reinforcement fiber to direct the desired radial expansion of air bladders. These soft robotic gloves could achieve active flexion and passive extension support with better compliance to the fingers. However, most of them are insufficient in abduction-adduction and opposition support, especially for the thumb.

The thumb abduction-adduction and opposition play an essential role in daily activities such as grasping and picking up objects of various sizes. Specifically, thumb opposition is the primary contributor of a more dexterous human hand [10] and is valued as 50% to 60% of thumb function [11]. Accordingly, a high functional hand rehabilitation device should provide full thumb flexion, abduction-adduction, and opposition support.

So far, most of the efficient thumb exoskeletons [12]–[16] consist of rigid mechanical systems. Soft-actuator-activated prosthetic hand [17] could perform thumb oppositions, but it would be less applicable for real hand support since it was not designed with full consideration of a real thumb's biomechanical characteristics. Soft robotic gloves that concerned thumb opposition support used two approaches: *Separate actuators* for the thumb flexion and abduction support; For example, for thumb abduction support, Jiralerspong *et al.* [18] designed a unique V-shaped actuator, Wang *et al.* [19], Hu *et al.* [20], and Li *et al.* [21] minimized their thumb flexion actuators into a small segment and arranged them transversely between the thumb and the index finger. These separate actuators could transform the actuating force efficiently to the thumb since their deformation direction is in accordance with the thumb movement for which they are responsible. Nevertheless, these studies ended with the abduction actuators generating a very small force (i.e., 0.9 N at 50 kPa air inflation [18]) without further discussing their optimum design. Moreover, to realize part of grasping with multiple DoFs, actuators were designed to have an initial angle larger than the minimum angle formed between the 1st and the 2nd metacarpal bones. Therefore, they limited the thumb abduction and opposition range (the thumb is impossible to contact positions close to the palm). As another solution, few soft robotic gloves used *one single-chamber actuator* with a specially designed corrugated fabric layer [7], [22] and reinforcement fiber [8], [23] to realize the opposition support. These opposition actuators can achieve a specific opposition motion path; However, they cannot adjust the flexion and abduction

separately, thus limited the RoM of thumb opposition. Yet, hardly any studies used soft actuators to support a full range of thumb opposition, which requires the coordination of a complete flexion and abduction support.

The difficulties for full functional thumb support lie in the intrinsic complexity of thumb movements and spatial constraints of the hand's dorsal side. Specifically, Multiple actuators that support movements in different directions need to be arranged within a restricted space between the 1st and the 2nd metacarpal bones. Also, the interference among either the multiple soft actuators with single DoF or multiple DoFs within one soft actuator would deviate the thumb movement from the desired one. Consequently, the existing prototypes of soft robotic gloves mainly enabled one-DoF support.

In order to achieve a more functional hand assist, this study aimed to design soft actuators for the thumb abduction-adduction and opposition support. We optimized the two aforementioned approaches: to combine two independent soft actuators for thumb abduction-adduction support and flexion support, respectively (combination approach), and to use one single soft actuator to assist motions in different directions (all-in-one approach). We designed two types of soft actuators, for which contrasting models were constructed and compared. The fan-shaped actuator (fan-ACT) for thumb abduction was designed with consideration of the hand's spatial constraint and actuator's thickness expansion restriction. The 3-chamber actuator (3C-ACT), a slender actuator with three chambers, has an inner structure designed based on the unique RoM requirement of thumb joints. Multi-chamber structured soft actuators have been well studied as surgery devices, which are required to have high flexibility, with less requirement of force output (less than 1 N [24]). 3C-ACTs in this study aimed to be multi-DoFs and have a considerable force output, taking into consideration of the biomechanical characteristics of thumb.

Actuators' abduction and flexion performances were assessed by RoM and force output; opposition performance was evaluated by an enhanced Kpandji test that measured both the Kapandji score and pinching strength concerning practical hand rehabilitation. We aimed to find out: (1) the optimum design of each approach; (2) the more effective thumb assistive approach through comparisons within each approach and between approaches.

II. THUMB SUPPORT APPROACHES

For ease of discussion, thumb opposition could be divided into 2 phases: In phase one, the metacarpal abducts; In phase two, the abducted metacarpal flexes and medially rotates toward other fingers [25]. Rotation of the metacarpal bone is not considered a third DoF as it cannot be performed independently of the other motions. Accordingly, we focused on assisting two DoFs: active flexion and active abduction.

RoM requirements were set based on the RoM of a healthy participant's left thumb (Table I). Active thumb extension was not considered since the thumb rehabilitation exercises mainly involved active flexion, with finger extension be practiced separately.

A. Combination Approach: Fan-Shaped Actuator

Design concepts of the fan-ACTs: Intrinsic muscles responsible for thumb abduction and opposition are mainly located between the 1st and the 2nd metacarpals (Fig. 1(A)). They apply

TABLE I
ROM OF THUMB JOINTS AND ROM REQUIREMENTS

Joint	Motion	Measured (°)	Requirement (°)
IP	Extension/Flexion	- / 90	90
MCP	Extension/Flexion	- / 37	37
CMC	Extension/Flexion	60 / 15	0 / 15
CMC	Abduction	60	60

RoM: range of motion, IP: interphalangeal, CMC: carpometacarpal, PIP: interphalangeal, MCP: metacarpophalangeal.

(A) Morphology of hand muscles (B) Spatial constrain

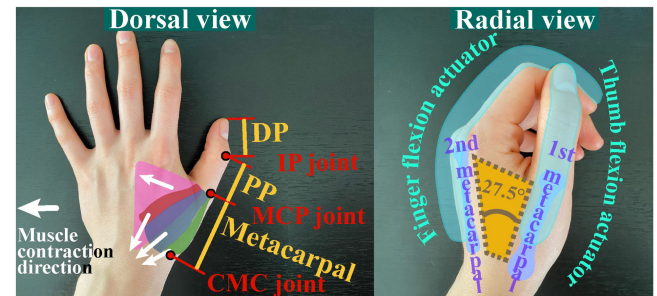


Fig. 1. The morphology of hand muscles (A, marked in different colors) and the spatial constraint of the hand's dorsal side (B).

forces directly to the thumb's MCP joint and the 1st metacarpal bone [25], [26]. This triangular area maintains flat either when the thumb rests in the same plane of the palm or when it rests facing the ulnar side of the palm (Fig. 1(B), marked in yellow). Moreover, soft actuators of rehabilitation gloves are mounted on the dorsal side of finger digits and usually in length from the middle of the metacarpal to the fingertip [9], therefore, leaving this triangular area available for an extra abduction actuator.

Two models of fan-ACTs were designed to mimic the muscle group's triangular shape and force application mechanism to maximize usage of the confined space (Fig. 2). The focus was putting on coordination with a flexion actuator to achieve the thumb opposition.

Model A: Middle-hole model. The actuator consists of three parts: a core unit, a thickness expansion restrictor, and two holding frames (Fig. 2(A)). The core unit takes the shape of an annulus sector with the sector angle set as 27.5°, which equals the natural angle formed by the 1st and the 2nd metacarpal bones when the hand rests with the palm's lateral side facing upward (Fig. 1(B)). An elliptic hole was positioned on the actuator unit's symmetry axis for fixing the thickness expansion ring. Reinforcement fiber was coiled longitudinally in two-directional hitching [9], with knots arranged at the shorter arc, to the actuator surface in a 3° interval. The two holding frames were connected in a ball joint connection, which makes the actuator open like a fan and be bendable to permit the extreme flexion of the thumb.

Model B: 2-segment model. To minimize the thickness expansion and make the fan-ACT more bendable to coordinate with a flexion actuator, we divided the core unit of Model A into two segments (Fig. 2(B)) aligned with the symmetry axis. Reinforcement fiber was coiled to the two segments separately. An air tube was threaded through the two segments, thereby enabling simultaneous inflation.

abduction-adduction of the lower half of the actuator. Finally, the root part of the actuator was designed to be a plastic connector that enabled the actuator to connect to the dummy finger or a supporting orthotic structure on the hand (Fig. 3(D and E)).

Model 2: Semi-cylindrical 3C-ACT with tapering chambers. This 3C-ACT was in a tapering structure designed based on the unique RoM requirements of the thumb. Generally, the thumb's CMC joint, a saddle joint at the root, has a larger RoM of abduction than flexion [27]; therefore, it requires a more intensive force to impel abduction rather than to flex it. On the contrary, the thumb's IP joint, a hinge joint at the tip, has the maximum flexion RoM of the three thumb joints [27], requiring more force for flexion but not for abduction. Accordingly, the two side chambers for abduction-adduction were designed in a tapering down fashion (the maximum cross-sectional area at the root and the minimum at the tip). The middle chamber for flexion support was in tapering up fashion (Fig. 3(B)).

Model 3: Cuboid 3C-ACT with tapering chambers. An actuator's bending performance would be affected by the deformation of the chamber wall opposite to the bending direction. The cuboid actuator has larger sidewalls opposite the abduction and adduction direction, making it suitable for thumb abduction-adduction support. Therefore, we revised Model 2 to a cuboid actuator. The middle chamber remained the same. The side chambers have the same cross-sectional area as Model 2 but in an elliptic shape (Fig. 3(C)).

C. Actuator Fabrication

Actuators were fabricated using molds that printed out with 3D-printer (Ultimaker 2 Extended+, Ultimaker B.V., Netherland) using PLA filament. Dragonskin 10 Slow and 20 (Smooth-On, Inc., US) were used to fabricate the main body of fan-ACTs and 3C-ACTs, respectively; and Ecoflex 00-30 for the final coating to fix the reinforcement fibers (cotton thread, 0.7mm, Shinwa Rules Co., Japan).

All the rigid accessories, namely, the holding frames and thickness expansion restrictor of the fan-ACT and the root connector of the 3C-ACT, were printed out by 3D printers.

III. EVALUATION

Thumb assist performances of the designed actuators were evaluated in terms of RoM and force output of flexion and abduction, and an enhanced Kapandji test [28] for assessing not only the kinematic aspect of opposition but also the pinching strength exerted by the actuators. A dummy hand mimicking the participant's hand was prototyped for most of the evaluations. It consists of a palm that was simplified into a rectangular block and five bendable finger digits. Air was inflated to each actuator's extreme air pressure and deflated with a 10-kPa interval. Each measurement was repeated two times, and the average was calculated.

A. RoM Measurement

RoMs were measured using a 2-dimensional motion capture system (GigE Monochrome Camera System GE60, Library, Japan). The camera was set in front of the movement plane and perpendicular to it (Figs. 4(A) and 4(B)).

The 3C-ACTs might not directly abduct when inflating the side chamber but flex concurrently due to the interaction between chambers constrained in a common silicon body. Therefore, we

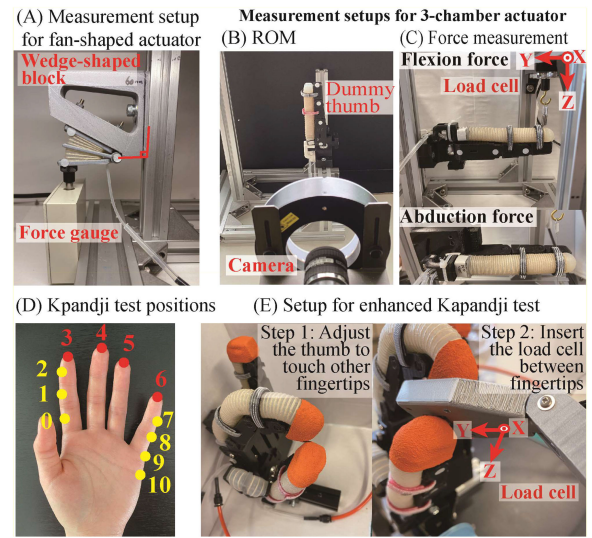


Fig. 4. Measurement setups.

measured the RoM and force of both flexion and abduction during the inflation of the left side chamber.

B. Force Output Measurement

The abduction force of fan-ACTs was measured using a force gauge (DPU-50N, IMADA, Japan) (Fig. 4(A)). The flexion and abduction force of 3C-ACTs were measured using a 3-axis load cell (USL06-H5 Load cell, maximum: 100N, Tec Gihan, Japan, Fig. 4(C)). The flexion force generated at the middle of each segment, including the distal phalanx (DP), proximal phalanx (PP), and metacarpal, was calculated as the net force of F_Y (actuator elongation force) and F_Z (actuator flexion force). The overall abduction force of 3C-ACTs was measured at the middle of the DP segment since the abduction only occurs at the CMC joint. F_Z was the abduction force, and the net force of F_X (actuator flexion force) and F_Y (actuator elongation force) was the flexion force during an abduction.

C. The Measurement of Enhanced Kapandji Test

Kapandji score ranges from 0 to 10 (Fig. 4(D)), depending on where the tip of the thumb could touch. Position 10 was omitted because it is hard to reach even for a healthy hand. Flexion actuators were in a semi-cylindrical single-chamber structure with the same width and height as the 3C-ACT.

For the pinching strength measurements, we first made the two fingertips contact, then inserted the 3-axis load cell between fingertips to record the change of pinching strength with the increase of air pressure in the two flexion actuators (Fig. 4(E)). Air inflation of each flexion actuator was increased with an interval of 10 kPa until its maximum air pressure (at which the actuator twisted). The pinching strength was calculated as the net force of F_X , F_Y , and F_Z .

IV. RESULTS

A. Results of Abduction and Flexion Measurements

We analyzed inflation and deflation data separately when there was a great difference between the two and analyzed the average of both when the difference was not significant.

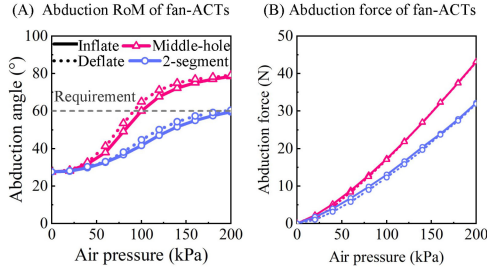


Fig. 5. Abduction RoM (A) and force (B) of fan-shaped actuators.

Fan-ACTs: abduction RoM and force. Both fan-ACT models achieved the required abduction RoM (60°) (Fig. 5(A)). The middle-hole model had a larger abduction angle and force output (43 N, Fig. 5(B)).

3C-ACTs: flexion RoM and force. The flexion RoM result showed that only Model 2 flexed each joint close to the requirement (Fig. 6). In contrast, the other two models were far from the requirement, especially for the IP joint.

The flexion force results (Fig. 7) showed that Model 2 generated the largest flexion force at three thumb segments. Notably, Model 1 showed a different flexion force distribution on the thumb compared with the other models; It generated the maximum flexion force at the PP (5.8 N) and less flexion force at the DP (4.1 N) and the metacarpal bone (4.0 N). In contrast, Model 2 and Model 3 generated the maximum flexion force at the DP, the medium at the PP, and the minimum at the metacarpal bone.

3C-ACTs: abduction RoM and force. All three models had an initial abduction angle of approximately 17° (Fig. 8(A)), which equals the intrinsic angle formed between the 1st and the 2nd metacarpal bones when the thumb adducted closely to the index finger.

Model 3, in a cuboid shape, abducted the CMC joint to 65° (Fig. 8(A)), which was larger than the requirement (60°). In contrast, the abduction angle of Model 2 was slightly less than the requirement, and that of Model 1 was far from satisfying the requirement. The abduction force also showed a similar tendency (Fig. 8(B)).

In addition, finger flexion was observed during the inflation of the side chamber. Generally, Model 3 flexed the least angle and Model 2 the most (Fig. 9(A-C)); Correspondingly, Model 2 generated the most flexion force, Model 3 the less, and Model 1 the least (Fig. 9(D)) during the side chamber inflation.

B. Results of the Enhanced Kapandji Test

Kapandji score results: Model A and Model B of fan-ACT achieved a score of 1–6 (Table II, supplementary video). Both models could not make the thumb contact the lateral side of the index finger’s PP segment (position 0) and the volar aspect of the small finger (position 7–9). In contrast, all three models of the 3C-ACT achieved a score of 0–8, greater than that of fan-ACTs. The thumb was difficult to reach position 9 due to the limitation of the dummy hand. Alternatively, we measured the distance between the thumb’s fingertip and the target position.

Pinching strength results: The pinching strength of fan-ACTs and Model 2 and Model 3 of the 3C-ACTs is shown in Fig. 10. The thumb generated various pinching strength levels with different fingers when using fan-ACTs (Fig. 10(A)). The pinching strength of thumb-index (finger) and thumb-middle (finger),

TABLE II
THE KAPANDJI SCORE OF EACH ACTUATOR (MM)

		Stage 1			Stage 2			Stage 3			
		0	1	2	3	4	5	6	7	8	9
Fan-ACT	Model A	×	✓	✓	✓	✓	✓	✓	×	×	×
	Model B	×	✓	✓	✓	✓	✓	✓	×	×	×
	Model 1	✓	✓	✓	✓	✓	✓	✓	✓	✓	×
3C-ACT	Model 2	✓	✓	✓	✓	✓	✓	✓	✓	✓	×
	Model 3	✓	✓	✓	✓	✓	✓	✓	✓	✓	×

×: The thumb’s fingertip cannot contact the target position; (): the distance in millimeter between the thumb’s fingertip and the target position; ✓: The thumb’s fingertip reached the target position; Fan-ACT: fan-shaped actuator; 3C-ACT: 3-chamber actuator.

fingers close to the thumb, was larger when using Model A. For the ring finger and the small finger that are relatively far from the thumb, Model B showed a larger maximum pinching strength due to a larger adjustable air pressure range of flexion actuators. In contrast, the pinching strength level did not vary much with fingers when using the 3C-ACTs (Figs. 10(B) and 10(C)). The semi-cylindrical Model 2 generally showed a greater pinching strength than the cuboid Model 3. The magnitudes of the maximum thumb-finger pinching strength were similar to that of the fan-ACTs.

V. DISCUSSION

A. Comparison Within Each Approach

In this section, we compared the models of the fan-ACT and 3C-ACT, respectively.

1) Comparison Between Fan-ACTs: Abduction performance: Both the middle-hole and 2-segment models of fan-ACT satisfied the RoM requirement for a full thumb abduction (Fig. 5). They generated an abduction force of more than 32 N, close to the maximum abduction force generated by the thumb of a healthy dominant hand (35 N [29]). Certainly, a force of this magnitude might be excessive to assist a healthy thumb to abduct, but it would be useful for assisting the thumb with high joint stiffness.

Opposition performance: The middle-hole and the 2-segment fan-ACTs had the same Kapandji score but showed different thumb-finger pinching strength. The single-chamber actuators for the thumb and finger flexion were identical during the pinching strength measurements. The two models would show similar pinching strength if they had a similar interaction with the thumb flexion actuator. However, the maximum pinching strength of the ring finger and the small finger, which requires greater thumb flexion to make the fingertips contact, were smaller when using the middle-hole model (Fig. 10(A)). This result suggested that the flexion force needed to compensate for the twist of the middle-hole model might be much bigger than that for the 2-segment model during the thumb opposition. To testify to this assumption, we measured the twisted angles of the two fan-ACTs, adding weights (0–5 N) on one of their holding frames when the actuators were inflated with the same air pressures as needed for the thumb-finger contact. The results showed that the 2-segment model twisted a larger angle than the middle-hole model at the same loading condition (the differences were 7 to 10° ,

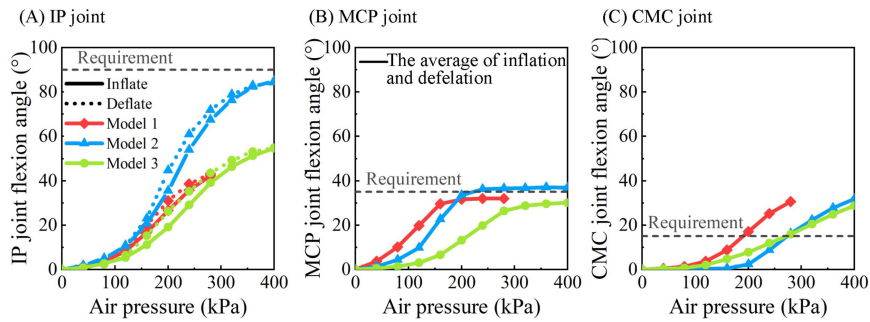


Fig. 6. Flexion RoM of (A) IP, (B) MCP, and (C) CMC joints when using 3-chamber actuators. IP: Interphalangeal joint, MCP: Metacarpophalangeal joint, CMC: Carpometacarpal joint.

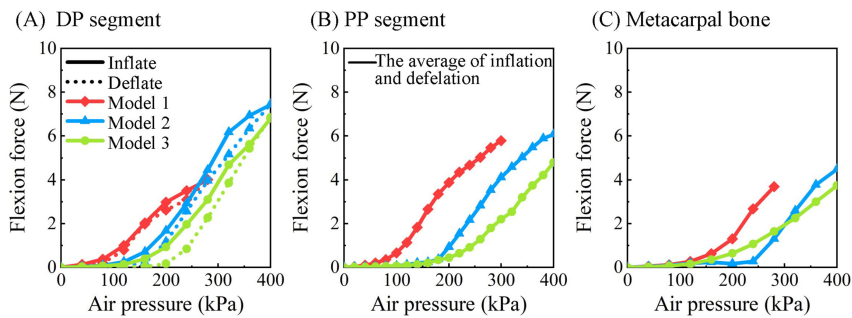


Fig. 7. Flexion force generated at the (A) DP, (B) PP, and (C) metacarpal bone when using 3-chamber actuators. DP: distal phalanx, PP: proximal phalanx.

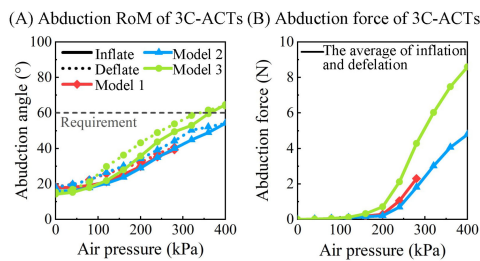


Fig. 8. Abduction RoM (A) and force (B) of 3-chamber actuators.

Appendix Fig. A). Structurally, the 2-segmented design reduced the core unit's thickness expansion more efficiently, making the actuator easier to be twisted. Therefore, the 2-segment fan-ACT could cooperate with the thumb flexion actuator with higher compliance, thus resulting in a greater pinching strength.

Generally, both fan-ACT models are applicable for thumb abduction support, but the 2-segment model is more suitable for opposition support.

2) *Comparison Among 3C-ACTs: Flexion performance.* Only Model 2, a semi-cylindrical actuator with tapering chambers, achieved an RoM close to a full thumb flexion (Fig. 6). It also generated a greater maximum flexion force at each thumb segment than the other two models. The maximum flexion force at the DP segment was approximately 7.4 N (Fig. 7(A)), which is larger than the minimum force for full flexion of finger joints (7 N, [30]). Therefore, only Model 2 has the potential of assisting a full thumb flexion.

It is noteworthy that the RoM and force during air deflation are usually larger than that during inflation, owing to the nonlinearity of silicon material. However, Fig. 7(A) showed a smaller force during air deflation. The reason for the reversed hysteresis would

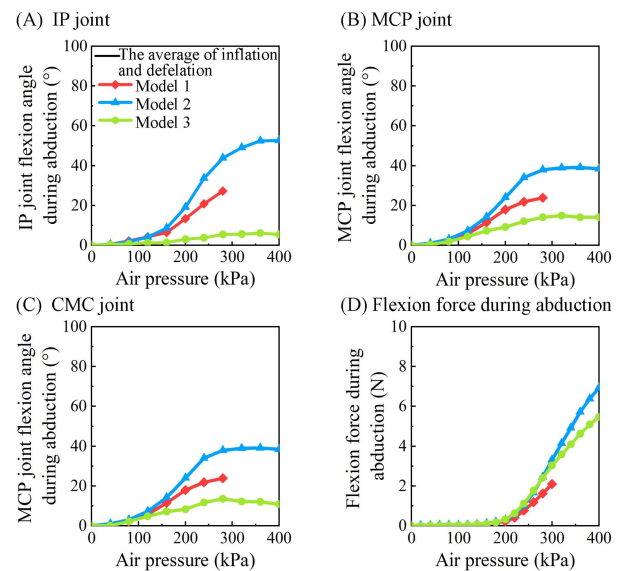


Fig. 9. Flexion RoM of the (A) IP, (B) MCP, and (C) CMC joint during thumb abduction; and (D) the overall flexion force during abduction when using 3-chamber actuators. IP: Interphalangeal joint, MCP: Metacarpophalangeal joint, CMC: Carpometacarpal joint.

be the use of a multi-joint dummy thumb. The bending of joints made the measured force a z-directional component force ($F \cdot \cos \theta$, refer to Fig. 4(C) for direction), and the joint angle θ would affect the magnitude of the measured value in an inverse proportional way.

In accordance with our design purpose, Model 2 and Model 3 with a tapering-up middle chamber generated the minimum

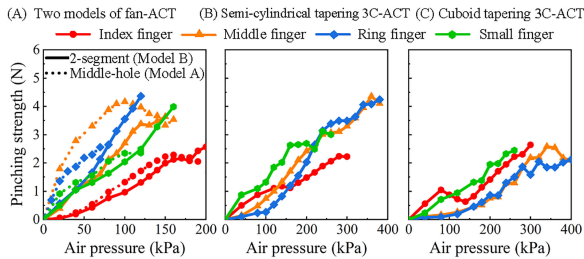


Fig. 10. Pinching strength of fan-ACTs and 3C-ACTs.

flexion force at the CMC joint and the maximum at the IP joint (Fig. 7), which indicated that the tapering-chamber design could implement thumb flexion support in compliance with the thumb's biomechanical characteristics.

In contrast, Model 1 with three constant chambers had the minimum flexion force at the CMC joint and the maximum at the MCP joint, which partially satisfied the other four-finger digits' requirements. The PIP joint of four-finger digits (corresponding to the thumb's MCP joint) has the largest flexion RoM requirement [27]. Accordingly, Model 1 might not be the optimum for thumb support; on the other hand, it might be suitable for assisting the flexion of four-finger digits.

Abduction performance: The abduction angle and force results showed that only Model 3, a cuboid actuator, satisfied the abduction angle requirement (Fig. 8), suggesting its potential of realizing a full thumb abduction assist.

Considering both abduction and its concomitant flexion, the cuboid Model 3 generated a larger force for abduction than flexion during the side chamber inflation (Fig. 8(B) v. Fig. 9(D)), whereas the semi-cylinder Model 2 the contrary, indicating that actuator in a cuboid shape has an advantage in abduction assistance compared with the semi-cylinder one.

Opposition performance: All three models achieved the same Kapandji score of 0–8 (Table II). Position 9 can be reached by only flexing the thumb. Model 2 and Model 3 with tapering chambers could flex to a similar height as position 9 when inflating the middle chamber to its maximum air pressure. However, they had a distance in the volar direction, which could be diminished if the metacarpal of the small finger of the dummy hand is bendable. In contrast, Model 1 could not flex to the height of position 9 due to its inferior flexion capability.

The semi-cylindrical Model 2 had a greater pinching strength than the cuboid Model 3 (Fig. 10(B) v. 10(C)), owing to its superior flexion performance. On the other hand, the maximum thumb abduction angle of practical opposition movements is approximately 42° (25° [31] added the initial angle of 17° measured in this study), less than the maximum abduction RoM of Model 3 (64° , Fig. 8(A)). So, its advantage in abduction did not fully exploit in opposition support.

Consequently, Model 3 might be more suitable to assist movements with large abduction requirements, such as grasping large objects. In contrast, Model 2 would be more applicable for the thumb opposition assist.

B. Comparison Between Two Approaches

The initial sector angle (27.5°) of fan-ACTs made them impossible to contact the positions close to the palm, resulting in a smaller Kapandji score than the 3C-ACTs (Table II). Also, a part of the flexion force generated by the thumb flexion actuator

would be consumed to twist the fan-ACT when reaching the ulnar part of the hand. Accordingly, the interference between independent actuators would impair their assistive effect, thus making the combination approach difficult to realize a full thumb opposition support. In contrast, the 3C-ACTs could achieve motions containing abduction and flexion effortlessly by first inflating the side chamber to abduct and flex the thumb to some extent, then inflating the middle chamber to flex the thumb further if necessary. Therefore, the negative interference between chambers might be less significant than that between independent actuators and thus make the full thumb opposition possible.

The superior model of the two approaches, 2-segment fan-ACT and Model 2 of 3C-ACT, generated similar levels of thumb-finger pinching strength (Fig. 10(A) and (B)). However, they might be suitable for different scenarios considering their overall performances.

The fan-ACT could generate an abduction force of more than 32 N (Fig. 5(B)), whereas the 3C-ACT only 4.5 N (Fig. 8(B)). Soft actuators often need to stretch fingers with severe joint stiffness [32] at the initial status of the robot-assisted rehabilitation. The 2-segment fan-ACT with a larger abduction force output would be preferable for the early rehabilitation stage.

The 3C-ACT could adjust a certain range of pinching strength within a wider air pressure range (Fig. 10(B)). In contrast, the pinching strength of the 2-segment fan-ACT would change intensively with the air pressure change in the flexion actuator. Accordingly, the pinching strength of the 3C-ACT could be controlled more precisely and subtly by adjusting air inflation, suggesting its potential of assisting fine motor movements, i.e., precision pinch.

VI. CONTRIBUTIONS AND LIMITATION

In this study, soft actuators were designed for realizing the thumb opposition with sufficient pinching strength for the first time in the research area. Our contribution can be summarized as follows:

About the realization: 1) Two approaches for thumb support were accomplished by biomimetic designs and systematically compared. 2) For the combination approach, multiple constraints (thickness expansion, spatial) were considered in prototyping, which is the first trial to deal with the difficulties due to the combination of multiple actuators for thumb support. 3) For the all-in-one approach, the design considerations accounting for multiple-chamber interaction that caused DoF differentiation and interference were first addressed in the soft actuator research area.

About findings: Both approaches were tested to be applicable for thumb support, and their practical usages in different hand rehabilitation stages were made clear.

Still, some tasks need to be further fulfilled. The primary task would be to evaluate the two approaches with dummy hands that can mimic a certain degree of impairment or hands of stroke patients. The semi-cylindrical and cuboid 3C-ACTs have advantages in supporting movements in different directions. Combining the two shapes' characteristics might develop an actuator good at both flexion and abduction support. Moreover, to realize a natural thumb opposition support, it would be necessary to develop the control method of multiple soft actuators (or air bladders) considering the interaction and interference between actuators (or chambers).

VII. CONCLUSION

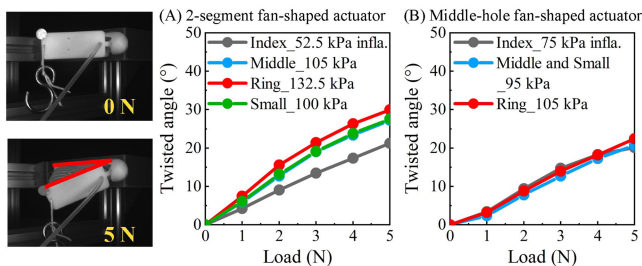
This study designed two types of actuators representing different thumb support approaches: The fan-ACTs need to coordinate with a thumb flexion actuator for thumb opposition support; The 3C-ACTs could assist both thumb abduction and flexion simultaneously. Each actuator type was designed with different models.

Both middle-hole and 2-segment fan-ACTs satisfied the abduction RoM and force requirement. However, the 2-segment model would be optimal for assisting the thumb opposition due to its higher compliance with the thumb flexion actuator.

Comparison among 3C-ACTs showed that the flexion force generated by Model 2 and Model 3 with tapering chambers were in accordance with the RoM requirements of a real thumb, whereas Model 1 with constant chambers did not, which testified the validity of the tapering-chamber design. Furthermore, the cuboid model 3 might be suitable for assisting abduction movements owing to its better abduction performance. The semi-cylindrical Model 2 is more applicable for thumb opposition rehabilitation due to its better flexion performance and intensive pinching strength.

Comparison between the two approaches indicates that the combination approach might be suitable for the early stage of rehabilitation due to its intensive abduction force output. The all-in-one approach could assist fine motor movements in the mid-late stage of rehabilitation for its higher Kapandji test score and its potential to control the pinching force exertion more subtly.

APPENDIX
FIGURE A



ACKNOWLEDGMENT

Yuanyuan Wang thanks The Iwatani Naoji Foundation for their financial support for her doctoral study.

REFERENCES

- [1] WSO, "Global stroke fact sheet," 2019. [Online]. Available: [Online]. Available: https://www.world-stroke.org/assets/downloads/WSO_Global_Stroke_Fact_Sheet.pdf
- [2] H. C. Fischer *et al.*, "Use of a portable assistive glove to facilitate rehabilitation in stroke survivors with severe hand impairment," *IEEE Trans. Neural Syst. Rehabil. Eng.*, vol. 24, no. 3, pp. 344–351, Mar. 2016.
- [3] J. M. Ochoa, Y. J. Dev Narasimhan, and D. Kamper, "Development of a portable actuated orthotic glove to facilitate gross extension of the digits for therapeutic training after stroke," in *Proc. IEEE Int. Conf. Eng. Med. Biol. Soc.*, 2009, pp. 6918–6921.
- [4] S. W. Lee, K. A. Landers, and H. - S. Park, "Development of a biomimetic hand exotendon device (BiomHED) for restoration of functional hand movement post-stroke," *IEEE Trans. Neural Syst. Rehabil. Eng.*, vol. 22, no. 4, pp. 886–898, Jul. 2014.
- [5] P. Polygerinos *et al.*, "Towards a soft pneumatic glove for hand rehabilitation," in *Proc. IEEE Int. Conf. Intell. Robots Syst.*, 2013, pp. 1512–1517.

- [6] H. K. Yap *et al.*, "A soft exoskeleton for hand assistive and rehabilitation application using pneumatic actuators with variable stiffness," in *Proc. IEEE Int. Conf. Robot. Autom.*, 2015, pp. 4967–4972.
- [7] H. K. Yap *et al.*, "A fabric-regulated soft robotic glove with user intent detection using EMG and RFID for hand assistive application," in *Proc. IEEE Int. Conf. Robot. Autom.*, 2016, pp. 3537–3542.
- [8] P. Polygerinos, K. C. Galloway, E. Savage, M. Herman, K. O. Donnell, and C. J. Walsh, "Soft robotic glove for hand rehabilitation and task specific training," in *Proc. IEEE Int. Conf. Robot. Autom.*, 2015, pp. 2913–2919.
- [9] T. V. J. Tarvainen *et al.*, "New layouts of fiber reinforcements to enable full finger motion assist with pneumatic multi-chamber elastomer actuators," *Actuators*, vol. 7, no. 2, pp. 1–18, Jun. 2018.
- [10] L. A. Jones and S. J. Lederman, *Human Hand Function*. Oxford, U.K.: Oxford Univ. Press, 2006, pp. 141–143.
- [11] A. D. Armstrong *et al.*, *Essentials of Musculoskeletal Care*, 5th ed. Rosemont, IL, USA: American Academy of Orthopaedic Surgeons, 2015, pp. 505–516.
- [12] F. Wang *et al.*, "Design and control of an actuated thumb exoskeleton for hand rehabilitation following stroke," in *Proc. IEEE Int. Conf. Robot. Autom.*, 2011, pp. 3688–3693.
- [13] P. Aubin *et al.*, "A pediatric robotic thumb exoskeleton for at-home rehabilitation: The isolated orthosis for thumb actuation (IOTA)," *Int. J. Intell. Comput. Cybern.*, vol. 7, no. 3, pp. 233–252, Jun. 2014.
- [14] O. Lamberg *et al.*, "Design of a thumb exoskeleton for hand rehabilitation," in *Proc. Int. Conv. Rehabil. Eng. Assist. Technol.*, Aug. 2013, pp. 1–4.
- [15] J. Iqbal *et al.*, "A novel exoskeleton robotic system for hand rehabilitation - Conceptualization to prototyping," *Biocybern. Biomed. Eng.*, vol. 34, no. 2, pp. 79–89, Dec. 2014.
- [16] P. Agarwal *et al.*, "Design, control, and testing of a thumb exoskeleton with series elastic actuation," *Int. J. Rob. Res.*, vol. 36, no. 3, pp. 355–375, Apr. 2017.
- [17] J. Zhou, J. Yi, X. Chen, Z. Liu, and Z. Wang, "BCL-13: A 13-DOF soft robotic hand for dexterous grasping and in-hand manipulation," *IEEE Robot. Autom. Lett.*, vol. 3, no. 4, pp. 3379–3386, Oct. 2018.
- [18] T. Jiralerspong, K. H. L. Heung, R. K. Y. Tong, and Z. Li, "A novel soft robotic glove for daily life assistance," in *Proc. 7th IEEE Int. Conf. Biomed. Robot. Biomechanics*, 2018, pp. 671–676.
- [19] J. Wang, Y. Fei, and W. Pang, "Design, modeling, and testing of a soft pneumatic glove with segmented pneunets bending actuators," *IEEE/ASME Trans. Mechatronics*, vol. 24, no. 3, pp. 990–1001, Jun. 2019.
- [20] D. Hu, J. Zhang, Y. Yang, Q. Li, D. Li, and J. Hong, "A novel soft robotic glove with positive-negative pneumatic actuator for hand rehabilitation," in *Proc. IEEE/ASME Int. Conf. Adv. Intell. Mechatronics*, 2020, pp. 1840–1847.
- [21] M. Li *et al.*, "A soft robotic glove for hand rehabilitation training controlled by movements of the healthy hand," in *Proc. 17th Int. Conf. Ubiquitous Robots*, 2020, pp. 62–67.
- [22] T. Wang *et al.*, "Programmable design of soft pneu-net actuators with oblique chambers can generate coupled bending and twisting motions," *Sensors Actuators, A Phys.*, vol. 271, pp. 131–138, Mar. 2018.
- [23] P. Maeder-York *et al.*, "Biologically inspired soft robot for thumb rehabilitation," *J. Med. Devices, Trans. ASME*, vol. 8, no. 2, Jun. 2014, pp. 1–3.
- [24] B. Zhang, C. Hu, P. Yang, Z. Liao, and H. Liao, "Design and modularization of Multi-DoF soft robotic actuators," *IEEE Robot. Autom. Lett.*, vol. 4, no. 3, pp. 2645–2652, Jul. 2019.
- [25] D. A. Neumann, *Kinesiology of the Musculoskeletal Syst.*, 3rd ed., St. Louis, MO, USA: Mosby, 2016, pp. 194–247.
- [26] H. Gray, *Gray's Anatomy*. London: Arcturus Publishing, 2013.
- [27] K. S. Lee and M. C. Jung, "Ergonomic evaluation of biomechanical hand function," *Saf Health Work*, vol. 6, no. 1, pp. 9–17, Mar. 2015.
- [28] K. Shiota *et al.*, "Enhanced kapandji test evaluation of a soft robotic thumb rehabilitation device by developing a fiber-reinforced elastomer-actuator based 5-digit assist system," *Rob. Auton. Syst.*, vol. 111, pp. 20–30, Jan. 2019.
- [29] F. Liu *et al.*, "Quantitative abductor pollicis brevis strength testing: Reliability and normative values," *J. Hand Surg. Am.*, vol. 25, no. 4, pp. 752–759, Jul. 2000.
- [30] T. H. Yang *et al.*, "Assessing finger joint biomechanics by applying equal force to flexor tendons in vitro using a novel simultaneous approach," *PLoS One*, vol. 11, no. 8, pp. 1–13, Aug. 2016.
- [31] T. Kuroiwa *et al.*, "A new method of measuring the thumb pronation and palmar abduction angles during opposition movement using a three-axis gyroscope," *J. Orthop. Surg. Res.*, vol. 13, no. 1, pp. 1–8, Nov. 2018.
- [32] E. A. Chapman, "Joint stiffness: Effects of exercise on young and old men," *J. Gerontol.*, vol. 27, no. 2, pp. 218–221, Apr. 1972.